

## HF propagation model reflected by frontal Es

Ichiro Tomizawa<sup>1\*</sup>, Kotaro Fujii<sup>1</sup>

<sup>1</sup>SSRE, Univ. of Electro-Comm.

We have developed the method to derive precisely both direction and speed of the frontal Es by using the HF Doppler observation network with multi-reflection points. Based on the analysis of this method we have shown that the HF Doppler variation due to the frontal Es can be described by the mirror reflection model instead of the scattering model. It is therefore concluded that the frontal structure of Es should have both the thin cross-section less than the diameter of the first Fresnel zone and the horizontal straight-line shape much more than the same diameter.

Keywords: sporadic E, frontal structure, HF propagation model

## Study of quantitative characteristics of ionospheric disturbances during solar flare with the SuperDARN Hokkaido radar

Daiki Watanabe<sup>1\*</sup>, Nozomu Nishitani<sup>1</sup>

<sup>1</sup>Solar-Terrestrial Environment Laboratory, Nagoya University

Ionospheric disturbances during solar flare events have been studied by various kinds of observation instrument in the last few decades. Kikuchi et al. (1985) reported on the positive Doppler shift in the HF Doppler system data during solar flare events, and indicated that there are two possible factors of Doppler shift, i.e., (1) apparent ray path decrease by changing refraction index due to increasing electron densities in the D-region ionosphere, and (2) ray path decrease due to descending reflection point associated with increasing electron density in the F-region ionosphere.

In this study, we use the SuperDARN Hokkaido Radar to investigate the detailed characteristics of solar flare effects on ionospheric disturbances. We focus on positive Doppler shift of ground / sea scatter echoes just before sudden fade-out of echoes. Davies et al. (1962) showed that if the factor (1) is dominant, Doppler shift should have positive correlation with slant range and negative correlation with elevation angle and frequency. On the other hand, if the factor (2) is dominant, Doppler shift should have negative correlation with slant range and positive correlation with elevation angle and frequency. While Kikuchi et al. (1985) studied solar flare events and mainly discussed frequency dependence of Doppler shift, We study mainly slant range and elevation angle dependence, for the first time to the best of our knowledge. We found that the factor (1), in other words, increase of electron densities at D-region ionosphere, is dominant during solar flare events. This result is consistent with that of Kikuchi et al. In order to confirm this result and to study characteristics of ionospheric disturbance in more detail, we are working on the classification of solar flare events according to its intensity, local time, season and solar zenith angle, and the investigation of their effects on the ionospheric disturbances. We estimated variation of electron densities at D-region ionosphere and will estimate that of F-region ionosphere. In addition, we are trying to estimate variation of ionospheric electron densities by chemical reaction model using X-ray / EUV irradiation data from GOES and SDO satellites. We will compare the variation of ionospheric electron densities obtained from SuperDARN Radar data and that obtained from chemical reaction model. More detailed analysis result will be reported.

Keywords: solar flare, SuperDARN hokkaido radar, lower ionosphere, F-region ionosphere, Doppler shift

## The response of The 20 May 2012 solar ecliption the geomagnetic field

Takayoshi Oba<sup>1\*</sup>, Toshiaki, Mishima<sup>2</sup>, Satoru, Yamaguchi<sup>2</sup>, Yusuke, Oda<sup>2</sup>, Akiteru, Yamasaki<sup>2</sup>

<sup>1</sup>The Graduate University for Advanced Studies, <sup>2</sup>Osaka City University

The solar eclipse geomagnetic effect was studied ealier, but it was not clear so many.

We cannot distinguish geomagnetic effects due to an eclipse-induced from S<sub>q</sub> variation, because S<sub>q</sub> variation has irregularity depending on the day.

We need to evaluate the irregularity of S<sub>q</sub> variation to detect a disturbance during annular solar eclipse,when the effect expected is most discernible.

The annulation belt of the solar eclipse on 21 May 2012 run from the southwest of Japan to northeast,where the precise obsertational data gained in.

Creating a mathematical model through making reference to data of each observatory in Japan allow to presume the S<sub>q</sub> variation in Katano (KTN).

Some observatory has geomagnetic effect due to a solar eclipse and others don't have. Therefore, several mathematical models generate the residual having various signature.

In this paper, the results are compared with each other to detect a of annual solar eclipse.

Keywords: Geomagnetic effects, solar eclipse, Kalman filter

## Cause of long term variation of geomagnetic Sq field

Masahiko Takeda<sup>1\*</sup>

<sup>1</sup>Masahiko Takeda

Variation of geomagnetic Sq field amplitudes in the Y component at some observatories was studied and effect of the solar activity in the variation was investigated. While solar activity dependence of ionosphere conductivity could explain most solar activity dependence of the time scale for more than a few years of Sq amplitude, the solar activity dependence of the dynamo electric field was small. Rather, the dynamo field tends to be small when solar activity is high. Although there was a difference by an observatory in the long-term change of the a dynamo electric field, the difference is mainly due to the secular variation of a geomagnetic main field, and variation of the neutral wind velocity was almost the same at all observatories.

Keywords: geomagnetism, daily variation, solar activity, electric conductivity, neutral wind, main field strength

## Long-term variation in the upper atmosphere as seen in the geomagnetic solar quiet (Sq) daily variation

Atsuki Shinbori<sup>1\*</sup>, Yukinobu Koyama<sup>2</sup>, Masahito Nose<sup>2</sup>, Akiyo Yatagai<sup>1</sup>, Tomoaki Hori<sup>3</sup>, Yuichi Otsuka<sup>3</sup>

<sup>1</sup>RISH, Kyoto Univ., <sup>2</sup>DACGSM, Kyoto Univ., <sup>3</sup>STEL, Naogya Univ.

It has been well-known that geomagnetic solar quiet (Sq) daily variation is produced by the global ionospheric currents flowing in the E-region from middle latitudes to the magnetic equator. These currents are generated by dynamo process via interaction between the neutral wind and ionospheric plasma in a region of the lower thermosphere and ionosphere. The motion of the neutral particles is driven by heat convection due to solar irradiance and by tidal force of the sun and moon. According to the Ohm's equation, the ionospheric currents strongly depend on ionospheric conductivity, polarization electric field and neutral wind. Then, the long-term variations in the ionospheric conductivity and neutral wind in the lower thermosphere and ionosphere can be detected by investigating the long-term variation in the Sq amplitude. Recently, Elias et al. [2010] reported that the Sq amplitude tends to increase by 5.4-9.9 % in the middle latitudes in a period of 1961-2001. They mentioned that the long-term variation of ionospheric conductivity associated with geomagnetic secular variation mainly determines the Sq trend, but that the rest component is due to ionospheric conductivity enhancement associated with cooling effect in the thermosphere due to increasing greenhouse gas. In the present study, we try to clarify the characteristics of the long-term variation in the Sq amplitude using the long-term observation data of geomagnetic field and neutral wind. These observation data have been provided by Japanese institutes participating in the IUGONET (Inter-university Upper atmosphere Global Observation NETwork) project which started in FY 2009. In the present analysis, we used the F10.7 solar flux as a good indicator of the variation in the solar irradiance in the EUV and UV range as well as geomagnetic field data with time resolution of 1 hour observed at 184 geomagnetic stations. The definition of the Sq amplitude is the difference of the H-component between the maximum and minimum every day when the Kp index is less than 4. As a result, the long-term variation in the Sq amplitude at all the geomagnetic stations shows a strong correlation with the solar F10.7 flux which depends on 11-year solar activity. The relationship between the Sq amplitude and F10.7 flux was not linear but nonlinear. This nonlinearity could be interpreted as the decrease of production rate of electrons and ions in the ionosphere for the strong EUV and UV fluxes as already reported by Balan et al. [1993]. In order to minimize the solar activity dependence on the Sq amplitude, we calculated second orders of fitting curve between the F10.7 flux and Sq amplitude during 1950-2011, and examined the residual Sq amplitude defined as the deviation from the fitting curve. The residual Sq amplitude clearly shows increase and decrease trends with the periods of 20 years. It should be noted that the residual Sq amplitude around 2010 is almost the same level as that around 1970. On the other hand, the similar tendency can be seen in the diurnal variation of geomagnetic field in the auroral zone and polar cap (Sq<sub>p</sub> field) driven by the twin vortex of ionospheric currents associated with energy inputs from the solar wind into the ionosphere. Then, it seems that the trends in the residual Sq and Sq<sub>p</sub> fields are related to the long-term variation in the ionospheric conductivities associated with the secular variation of the ambient magnetic field and the upper atmosphere (for example, plasma and neutral densities). In order to verify qualitatively the above signatures, we need to investigate the long-term variation in the ionospheric conductivities using a calculation tool developed by the IUGONET project.

Keywords: Geomagnetic solar quiet (Sq) daily variation, Solar activity, Upper atmosphere, Neutral wind, Ionosphere, Thermosphere

## Plasma wave turbulence induced by the wake of an ionospheric sounding rocket

Ken Endo<sup>1\*</sup>, Atsushi Kumamoto<sup>1</sup>, Hiroshi Oya<sup>1</sup>, Takayuki Ono<sup>1</sup>, Yuto Katoh<sup>1</sup>

<sup>1</sup>Department of Geophysics, Graduate School of Science, Tohoku University

In the ionosphere, a rarefied plasma region called 'plasma wake' is formed behind a sounding rocket. For the past a few decades, many theoretical works, rocket experiments and numerical simulations have revealed the electron density depletion and the electron temperature enhancement in plasma wakes.

Several recent studies based on rocket observations have indicated that plasma waves are possibly excited in the rocket wake. They have discussed the observational results of the wave spectra in a frequency range around a few MHz based on the cold plasma theory and have suggested that the observed waves are the upper-hybrid resonance (UHR) mode waves. A wake turbulence model has been also proposed as a possible explanation for the waves where the two stream instability occurs in the wake center owing to the incident plasma flow from the both sides of the wake edges. However, there remains an issue that a part of the waves have not been explained by the dispersion relation of the UHR-mode waves calculated from the obtained electron density in the wake. In addition, these plasma waves have been investigated by using wave receivers with time resolutions worse than 500 msec, which is not enough for detailed investigations about their generations and propagations.

Plasma waves around the wake have been also reported in the region close to an artificial satellite and solar system bodies such as Moon. This suggests that the generation of plasma waves due to the rocket wake should be understood as a kind of universal phenomena in interactions between streaming plasma and a non-magnetic body.

To discuss the properties of the plasma waves caused around the rocket wake in more detail, we have measured the electron number density and electric fields of plasma waves in the mid-latitude ionosphere by an impedance probe and a plasma wave receiver, which were installed on the sounding rocket S-520-26. The time resolutions of the two instruments are about 260 msec, which corresponds to one fourth or one fifth of a spin period. The rocket was launched at Uchinoura in Kagoshima Prefecture, Japan, on January 12, 2012, and reached at an altitude of 298 km, approximately. We have observed plasma waves in the frequency range of 1.3-2.4 MHz (MF range) as well as in the frequency range below 0.9 MHz (LF range). The MF emissions are similar to the observed waves in the previous studies. Although the frequency range of the MF emissions is around the UHR frequency, we reveal that a component of the emissions are not explained by the dispersion relation of UHR-mode waves in the wake condition, which is deduced from the IGRF magnetic model and the data obtained by the impedance probe.

In this study, we discuss the mode of the observed plasma waves based the dispersion relation in a hot plasma. Assuming that the waves are generated around the wake near the rocket, we clarify that the MF emissions are explained by electrostatic cyclotron harmonics (ESCH) waves as well as the UHR-mode waves and that the LF emissions are electrostatic whistler-mode waves, because the wave length should be shorter than the size of the disturbed region. Besides, the analysis of the rocket attitude tells us that the both emissions are strongly observed only when the dipole antenna is in a certain direction. Moreover, we perform calculations of plasma dispersion relations numerically by assuming anisotropic velocity distribution functions including an electron beam or temperature anisotropy. As a result, positive linear growth rates are obtained in the wave number and frequency ranges of the electrostatic UHR-mode waves, ESCH waves and whistler-mode waves.

In this presentation, we compare the observational results with the obtained dispersion relations and discuss the properties of the observed plasma waves.

Keywords: wake, plasma wave, sounding rocket, ionosphere

## Observation of ionospheric disturbance using GPS, and evaluation of their impact on air navigation augmentation system

Naoki Omatsu<sup>1\*</sup>, Yuichi Otsuka<sup>1</sup>, Susumu Saito<sup>2</sup>, Kazuo Shiokawa<sup>1</sup>

<sup>1</sup>STEL, Nagoya Univ., <sup>2</sup>NAV Department, ENRI

In recent years, GPS has been utilized for navigation system for airplanes. Propagation delays in the ionosphere due to total electron content (TEC) between GPS satellite and receiver cause large positioning errors. In precision measurement using GPS, the ionospheric delay correction is generally conducted using both GPS L1 and L2 frequencies. However, L2 frequency is not internationally accepted as air navigation band, so it is not available for positioning directly in air navigation. In air navigation, not only positioning accuracy but safety is important, so augmentation systems are required to ensure the safety. Augmentation systems such as the satellite-based augmentation system (SBAS) or the ground-based augmentation system (GBAS) are being developed and some of them are already in operation.

GBAS is available in a relatively narrow area around airports. In general, it corrects for the combined effects of multiple sources of positioning errors simultaneously, including satellite clock and orbital information errors, ionospheric delay errors, and tropospheric delay errors, using the differential corrections broadcast by GBAS ground station. However, if the spatial ionospheric delay gradient exists in the area, correction errors remain even after correction by GBAS. It must be a threat to GBAS.

In this study, we use the GPS data provided by the Geographical Survey Institute in Japan. From the GPS data, TEC is obtained every 30 seconds. We select 6 observation points from 26.4 to 35.6 degrees north latitude in Japan, and analyze TEC data of these points from 2001 to 2011. Then we reveal dependences of Rate of TEC change Index (ROTI) on latitude, season, and solar activity statistically. ROTI is the root-mean-square deviation of time subtraction of TEC within 5 minutes. In the result, it is the midnight of the spring and the summer of the solar maximum in the point of 26.4 degrees north latitude that the value of ROTI becomes the largest. We think it is caused by plasma bubbles, and the maximum value of ROTI is about 6 TECU/min. Since it is thought that ROTI is an index representing the spatial ionospheric delay gradient, we can evaluate the effect of spatial ionospheric delay gradient to GBAS. More detailed results will be reported in this presentation.

Keywords: ionosphere, GPS, satellite navigation, GBAS, ROTI

## Effect of IMF-By on variations of ionospheric total electron content at mid-latitudes

Takashi Maruyama<sup>1\*</sup>, Hidekatsu Jin<sup>1</sup>

<sup>1</sup>National Institute of Information and Communications Technology

The primary factor that controls ionospheric total electron content (TEC) variation is solar UV/EUV radiations through direct and indirect processes. The direct effect is the ionization of the thermospheric neutral particles by EUV radiations with wavelengths ( $\lambda$ ) shorter than 102.5 nm. Virtually all photons of  $\lambda < 102.5$  nm are absorbed by photoionization and the absorbed energy splits into the photo-electron channel and the chemical energy channel (ion-electron pair) with the ratio that depends on the wavelength. Indirect effects of solar irradiance on the ionosphere are through the modification of the thermosphere. The recombination of ion-electron pair and the dissociation process of molecular oxygen ( $O_2$ ) by the Schumann-Runge continuum radiation ( $\lambda = 130-175$  nm) are the primary heat source of the thermosphere. Changes in temperature and composition of the neutral atmosphere, and the atmospheric circulation greatly affect the ionospheric electron density.

Because the relationship between the solar spectral irradiance and ionospheric TEC is highly complex, we applied an artificial neural network (ANN) technique that has a great capability of function approximation of complex systems to model solar irradiance effects on TEC. Three solar proxies,  $F_{10.7}$ , SOHO-SEM<sub>26-34</sub> EUV emission index, and  $MgII_{c-w-r}$  were the input parameters to the ANN representing activities at various heights and regions of the solar atmosphere (Maruyama, JGR 2010). Although the trained ANN prediction model was confirmed to work well to predict TEC variations, there remained some errors as easily expected from the fact that another channel of energy flow from the sun to the earth's ionosphere in the form of solar wind was not considered in the model. Thus, in the next step, we have examined effects of magnetic disturbance, which is a manifestation of solar wind magnetosphere energy coupling. For this purpose, the  $K_p$  index and several solar wind magnetosphere coupling functions were chosen as an additional input parameter to the ANN-TEC model and we obtained a substantial improvement in the TEC prediction when the preprocessed  $K_p$  index was used.

Somewhat minor but interesting effects on TEC variations are expected to emerge when major effects of solar irradiance and magnetic disturbance have been removed. We analyzed the time series of residual error by using a wavelet transformation, which revealed an error characterized by a period of approximately 27-30 days in the summer. Possible origins of the error having such a period are (1) insufficient modeling of solar activity effect, (2) lunar tidal forcing, (3) coupling with planetary waves in the lower atmosphere, and (4) solar wind effect other than geomagnetic disturbances. Regarding the first and second possibilities, the time series of the error amplitude did not synchronize with the solar rotational modulation of the activity or the lunar age. The third possibility may not be probable because the penetration of planetary waves up to ionospheric heights is suppressed during the summer. We examined solar wind effects in detail.

A various solar wind parameters and their combinations were examined. The best result was obtained when the IMF-By component and the solar wind velocity were included in the input space of the ANN and the residual error showing the 27-30 day period during the summer was removed. Parallel use of the solar wind magnetosphere coupling function further improved the model. Possible explanation of the IMF-By effect is discussed in terms of changes in the thermospheric general circulation pattern.

Keywords: TEC, IMF-By, artificial neural network



## Study of gravity waves generated from strong tropospheric convection over Brazil by using multi-point GPS-TEC data

Daisuke Fukushima<sup>1\*</sup>, Kazuo Shiokawa<sup>1</sup>, Yuichi Otsuka<sup>1</sup>, VADAS, Sharon L.<sup>2</sup>, Michi Nishioka<sup>3</sup>, Takuya Tsugawa<sup>3</sup>

<sup>1</sup>Solar-Terrestrial Environment Laboratory, Nagoya University, <sup>2</sup>NorthWest Research Associates, Inc., <sup>3</sup>National Institute of Information and Communications Technology

It has been suggested that gravity waves causing the ionospheric disturbances were secondary waves generated by dissipation of primary gravity waves in the mesopause region or lower thermosphere. Vadas and Liu (submitted to JGR, 2013) simulated primary gravity waves generated from deep convection over Brazil after 18 UT on 1 October, 2005. They showed that the primary gravity waves generated secondary gravity waves through their dissipation in the thermosphere. The horizontal phase velocity, period, and horizontal wavelength of the secondary gravity waves were 500-600 m/s, 2-3 hours, and 4000-5000 km, respectively. They propagated even to Antarctica, Africa, and Europe.

In this study, we investigated whether these simulated gravity waves were actually observed or not, by using the total electron content (TEC) observed by the multi-point GPS receivers in South America. TEC perturbations which are likely to be caused by the gravity waves were seen around 4 UT on 2 October, 2005 in the TEC data at Brasilia, Brazil. The period of the observed TEC perturbation is slightly different from the original gravity-wave period since the observed period contains the effect of the GPS satellite motion, which varies depending on satellites. Based on multi-satellite analysis, we infer that the phase front of the observed gravity wave is east-west direction. The horizontal phase velocity, period, and horizontal wavelength of the gravity wave calculated by using the difference of the apparent periods were 660 m/s, 2 hours, and 4600 km, respectively. These parameters are similar to those of simulated secondary gravity waves described above. In the presentation, we discuss the comparison between the observed and simulated gravity waves.

Keywords: gravity wave, GPS-TEC, tropospheric convection

## Observational results with the Tromsø sodium LIDAR from October 2012 to March 2013

Satonori Nozawa<sup>1\*</sup>, Taku D Kawahara<sup>2</sup>, Norihito Saito<sup>3</sup>, Takuo Tsuda<sup>4</sup>, Testuya Kawabata<sup>1</sup>, Masaki Tsutsumi<sup>4</sup>, Shin-ichiro Oyama<sup>1</sup>, Toru Takahashi<sup>1</sup>, Hitoshi Fujiwara<sup>5</sup>, Satoshi Wada<sup>3</sup>, Yasunobu Ogawa<sup>4</sup>, Ryoichi Fujii<sup>1</sup>

<sup>1</sup>STEL, Nagoya University, <sup>2</sup>Faculty of Engineering, Shinshu University, <sup>3</sup>RIKEN, <sup>4</sup>National Institute of Polar Research, <sup>5</sup>Faculty of Science and Technology, Seikei University

We have made observations of the neutral temperature as well as wind velocity in the polar MLT region (80-110 km) from October 2012 to now (probably March) using the sodium LIDAR installed at Ramjordmoen, Tromsø (69.6N, 19.2E), where the EISCAT radars, MF radar, meteor radar (NIPR), FPI, aurora imagers have been operated. This season is our 3rd season of observations using the sodium LIDAR at Tromsø. In late September and early October 2012, we made further improvements of the LIDAR system such as (1) achievement of higher laser power output (about 4W), (2) replacement of a dome with a glass window, (3) use of narrower iris-mask, and (4) PC monitoring of temperature of laser devices.

This talk will give an overview of results obtained with the sodium LIDAR over about 6 months (October 2012 - March 2013) during the 3rd season. We mainly operated the sodium LIDAR with a five-beam mode where the laser beam was transmitted simultaneously toward five directions (vertical, north, east, south, west). In addition to the five-beam operation, we operated the sodium LIDAR with a vertical (1-beam) mode, where the laser beam was transmitted vertically only, for about 1 hour each in the beginning and ending, since the noise level of the vertical receiver was significantly lower than the others due to sharpness of receiving backscatter laser echo. We will present variations of atmospheric waves, horizontal structure of the neutral temperature, comparison of wind velocity obtained with the LIDAR and the meteor radar, and simultaneous observational results with the EISCAT radars.

Keywords: Sodium LIDAR, Temperature variation, lower thermosphere, mesosphere, polar upper atmosphere, EISCAT

## Progress of the middle and upper atmosphere observations over Syowa station in the Antarctic

Takuji Nakamura<sup>1\*</sup>, Kaoru Sato<sup>2</sup>, Masaki Tsutsumi<sup>1</sup>, Takashi Yamanouchi<sup>1</sup>

<sup>1</sup>National Institute of Polar Research, <sup>2</sup>Graduate School of Science, the University of Tokyo

The Japanese Antarctic Research Expedition (JARE) has started the VIII-th six-year mid-term project in 2010, and the 52nd JARE departed in November 2010 commenced observations of the six-year project. The middle and upper atmosphere study in the VIII-th term, named as 'Global environmental change revealed by observing the Antarctic middle and upper atmosphere', is one of the sub-projects of the prioritized research project entitled 'Global warming revealed from the Antarctic'. PANSY (Program of the Antarctic Syowa MST/IS) radar, and a Rayleigh/Raman lidar system have been newly installed besides the existing radio and optical instruments such as an MF radar, HF radar (Super DARN radar), ionosondes, an OH spectrometer and an all-sky airglow imager in Syowa station, in order to clarify variabilities on the atmosphere from the ground to the upper atmosphere. Also installed was a millimeter wave spectrometer for profiling minor constituents.

PANSY radar is the core instrument of this project, and is a 47 MHz VHF radar with 500 kW output power and 20,000 m<sup>2</sup> antenna array. The radar observes wind velocities from the troposphere to the mesosphere, as well as plasma parameters in the ionosphere. Three groups of antenna (1/18 of full system) was installed during summer operation of the 52nd JARE, and started observation of troposphere. Scientific observation with 12 groups of antenna (about 1/4) started since April 2012 and the tropospheric and lower stratospheric winds has been measured continuously. PMSE (Polar mesosphere summer echo) and PMWE (Polar mesosphere winter echo) have been monitored in detail by continuous observations. The Rayleigh/Raman lidar observes temperature and clouds in the mesosphere, the stratosphere and part of the troposphere, and providing data of gravity wave characteristics in the middle atmosphere, as well as high altitude clouds of PMC (polar mesospheric clouds) and PSC (polar stratospheric clouds). In order to extend the height coverage to include mesosphere and lower thermosphere region, and also to extend the parameters observed, an external laser system for multi-wavelength resonance scatter lidar measurement is being developed. The millimeter spectrometer measures density profiles of O<sub>3</sub> and other species. Since January 2012, NO density has been measured in order to observe day-to-day variation, in order to investigate NO variations due to high energy particles and electrons. Current status of the research and observations, as well as future plans will be presented in the presentation.

Keywords: Antarctic, Middle atmosphere, Upper atmosphere, radar observation, lidar observation, millimeter wave spectrometer

## Program of the Antarctic Syowa MST/IS Radar (PANSY) – after one year continuous operation since 2012 –

Kaoru Sato<sup>1\*</sup>, Masaki Tsutsumi<sup>2</sup>, Toru Sato<sup>3</sup>, Takuji Nakamura<sup>2</sup>, Akinori Saito<sup>3</sup>, Yoshihiro Tomikawa<sup>2</sup>, Koji Nishimura<sup>2</sup>, Masashi Kohma<sup>1</sup>, Hisao Yamagishi<sup>2</sup>, Takashi Yamanouchi<sup>2</sup>

<sup>1</sup>The University of Tokyo, <sup>2</sup>National Institute of Polar Research, <sup>3</sup>Kyoto University

The PANSY radar is the first Mesosphere-Stratosphere-Troposphere/Incoherent Scatter (MST/IS) radar in the Antarctic region. It is a large VHF monostatic pulse Doppler radar operating at 47 MHz, consisting of an active phased array of 1,045 Yagi antennas and equivalent number of transmit-receive modules with total peak output power of 500 kW. Its first stage has been installed at Syowa Station (69°00'S, 40°35'E) in early 2011, and is currently operating with 228 antennas and modules. This paper reports its scientific objects, technical descriptions, and preliminary results of observations made so far. The radar aims to clarify the role of atmospheric gravity waves in important polar events such as polar mesospheric clouds (PMC) and polar stratospheric clouds (PSC). The generation mechanism of gravity waves from katabatic winds is also of special interest. Moreover, strong and sporadic energy inputs from the magnetosphere by energetic particles and field-aligned currents can be quantitatively assessed by the broad height coverage of the radar extending from the lower troposphere to the upper ionosphere. From engineering points of view, the radar had to overcome restrictions due to severe environments of Antarctic research, such as very strong winds, limited power availability, and short period of construction with small manpower. We cleared these problems with specially designed class-E amplifier, light-weight and tough antenna elements, and versatile antenna arrangements. Although the radar is operating with only about a quarter of the full system, we have already obtained interesting results on the Antarctic troposphere, stratosphere and mesosphere, such as observation of gravity waves and multiple tropopause associated with a severe snow storm in the troposphere and stratosphere, and polar mesosphere summer echo.

Keywords: MST/IS radar, Antarctic atmosphere, Troposphere, Stratosphere, Mesosphere, Ionosphere

## Study on thermospheric sodium layer using Na lidar data from Syowa Station in Antarctica

Takuo Tsuda<sup>1\*</sup>, Xinzhao Chu<sup>2</sup>, Takuji Nakamura<sup>1</sup>, Mitsumu Ejiri<sup>1</sup>, Taku D Kawahara<sup>3</sup>

<sup>1</sup>National Institute of Polar Research, <sup>2</sup>University of Colorado, <sup>3</sup>Faculty of Engineering, Shinshu University

The neutral metallic atom layers (such as sodium, iron, potassium layers) are normally distributed at a height range of 80-110 km (in the upper mesosphere and lower thermosphere). Resonance scattering lidar observations of these metallic layers have been used as an important tool for investigation of the upper mesosphere and lower thermosphere. On the other hand, ground-based observations of the neutral atmosphere at higher altitude (above 110 km) are quite limited. Recently, observations of iron layers above 110 km up to 155 km have been reported from an iron Boltzmann lidar at McMurdo Station (77.8S, 166.7E) in Antarctica. Such high-altitude metallic layers (so-called thermospheric metallic layers) is currently well-unknown phenomenon, and has possibility to greatly improve our understanding of the lower thermosphere.

Intensive sodium temperature lidar observations were carried out at Syowa Station (69.0S, 39.6E) in Antarctica between 2000 and 2002 as a part of JARE observations. From the observational data, we investigate thermospheric sodium layer (above 110 km). In this presentation, we will report a thermospheric sodium layer event (up to 130 km) observed on 23 September 2000. In this event, the lidar detected significant signals not only from 80-110 km but also from 110-130 km. More detailed analysis has provided the temperature and the sodium-density measurements at this height range up to 130 km. The estimated sodium density reached about tens of  $\text{cm}^{-3}$  at around 120 km. The temperature profile in the thermospheric sodium layer was fairly comparable to that from the NRLMSISE-00 model. Furthermore we will discuss relationship between the thermospheric sodium layer and background ionospheric condition during the event.

Keywords: Sodium layer, Thermosphere, Syowa Station, Antarctica

## Variation of Nitric Oxide in MLT region associated with energetic particle precipitation

Yasuko ISONO<sup>1\*</sup>, Akira Mizuno<sup>1</sup>, Tomoo Nagahama<sup>1</sup>, Mitsumu Ejiri<sup>2</sup>, Ryuho Kataoka<sup>3</sup>, Masaki Tsutsumi<sup>2</sup>, Takuji Nakamura<sup>2</sup>, Hiroyuki Maezawa<sup>4</sup>, Yoshizumi Miyoshi<sup>1</sup>

<sup>1</sup>Solar-Terrestrial Environment Laboratory, Nagoya University, <sup>2</sup>National Institute of Polar Research, <sup>3</sup>Tokyo Institute of Technology, <sup>4</sup>Osaka Prefecture University

Energetic particle precipitation (EPP) due to large solar proton events or geomagnetic storms induces ion-molecule reactions and changes abundances of some minor molecules in the lower thermosphere, the mesosphere and the upper stratosphere. Energetic solar protons directly enter the middle atmosphere, causing increase of HO<sub>x</sub> and NO<sub>x</sub> radicals and decrease of ozone (e.g., *Lopez-Puertas et al. 2005*). Energetic electrons also increase NO<sub>x</sub> in the thermosphere, and the NO<sub>x</sub>-rich air is transported downward in the polar vortex during the polar winter (e.g., *Seppala et al. 2007*). To understand the variation mechanism of those molecules related to the solar activities and the polar vortex in the MLT region, we newly installed a microwave spectroscopic radiometer at Syowa Station in Antarctica (69.00S, 39.85E). We have been carrying out the ground-based continuous monitoring of microwave NO (250.796 GHz) spectral lines since January 2012, and 189 daily averaged NO spectra have been obtained.

Typical rms noise of the NO spectra is estimated 21 mK. Most of the spectra have been fitted by a single Gaussian with a half-power band width (HPBW) of 0.5 MHz, suggesting that the NO-line emitting region is lower thermosphere or mesosphere. The total intensity of NO emission shows a long-term or seasonal variation that increases more than a factor of two during a period from autumn to winter. The period of NO enhancement roughly corresponds to the polar vortex activity that are observed by CO downward descend obtained by MLS, but there is no significant increase of the line width of NO, suggesting that NO enhanced air mass does not reached down below ~60km. On the other hand, energetic electron precipitation events observed by GOES occurred more frequently during the NO long-term enhancement. The temperature below 100 km did not show significant variation throughout the observed period based on the SABER data, suggesting that the temperature variation did not affect on the NO total intensity. Thus, the enhancement of the NO total intensity reflects actual enhancement of NO column density. In addition to the long-term variation, we have detected short-term variations with a timescale of several days directly related with the energetic electron precipitation caused by large geomagnetic storms. The NO total intensity peaks during the recovery phase of the geomagnetic storms about 2-7 days after the main phase.

In this presentation, we will discuss about possible cause of the NO enhancement by comparing with satellite data such as SABER, GOSE, POES and MLS.

Keywords: microwave spectroscopy, Nitric Oxide, MLT region, Energetic Particle Precipitation

## Concentric rings of gravity waves in the mesosphere observed by the OMTI network in Japan

Shin Suzuki<sup>1\*</sup>, Kazuo Shiokawa<sup>1</sup>, Yuichi Otsuka<sup>1</sup>

<sup>1</sup>Solar-Terrestrial Environment Laboratory, Nagoya University

Atmospheric gravity waves significantly contribute to the wind/thermal balances in the mesosphere and lower thermosphere (MLT) through their vertical transport of horizontal momentum. It has been reported that the gravity wave momentum flux preferentially associated with the scale of the waves; the momentum fluxes of the waves with a horizontal scale of 10-100 km are particularly significant.

Airglow imaging is a useful technique to observe two-dimensional structure of small-scale (<100 km) gravity waves in the MLT region and has been used to investigate global behaviour of the waves. Solar-Terrestrial Environment Laboratory, Nagoya University has made long-term airglow imaging observations in the world using the Optical Mesosphere and Thermosphere Imager (OMTI) system. On 10 December 2002, concentric rings of gravity waves were observed simultaneously by all-sky imagers of OMTI in Japan located at Shigaraki (34.9N, 136.1E), and Rikubetsu (43.5N, 143.8E). The airglow structures, which were well-defined and formed a coherent wave pattern expanding from the southeast, were identified over 8 hours (1235-2047 UT or 2135-2947 LT). This unique event will give us new insight into the lower and upper atmosphere coupling.

In the presentation, we will report initial results on the concentric gravity waves on 10 December 2002 and discuss their possible source in the lower atmosphere.

## A study of the tidal periodicity of gravity wave energy in the mesosphere observed with MF radar at Poker Flat, Alaska

Takenari Kinoshita<sup>1\*</sup>, Yasuhiro Murayama<sup>1</sup>, Seiji Kawamura<sup>1</sup>

<sup>1</sup>NICT

The neutral wind velocity data from mesosphere to lower thermosphere observed by Poker Flat MF radar has been observed since October 1999. The National Institute of Information and Communications Technology (NICT) is developing science application software and database systems associated with remote sensing experiments, which include Poker Flat MF radar, and has been conducting scientific studies. A number of observational and theoretical studies have shown that a mesospheric meridional circulation which flows from the summer hemisphere to the winter hemisphere is mainly driven by gravity waves. On the other hand, the interaction between gravity waves and tidal waves has been studied by using observation and modeling data. However, the time and spatial variation of middle atmosphere general circulation has not been fully understood when the interaction processes are incorporated.

The purpose of this study is to improve the understanding of three dimensional (3D) structure of mesospheric circulation modified by gravity waves and tidal waves from observation and modeling data. First, we extracted tidal waves and gravity waves from the MF radar observation data. In this study, harmonic analysis was carried out for periods of 48, 24, 12, and 8 hours, which are extracted from the 5 day time series of wind velocity using. Gravity waves are defined as the 1 ~ 12 hour period component of difference between observed wind velocity and these harmonic components. The method is applied to 30-minute-average data to calculate the 5 day running mean amplitude and phase of tidal waves. We made 1-day composite plots of kinetic energy of gravity waves for periods of 1 ~ 4 hours and harmonic components. The results show that the kinetic energy of gravity waves has two peaks in 3 ~ 6 LT and 12 ~ 15 LT respectively, which tend to coincide with the time when easterly wind of the 12 hour component is switched westerly. This feature commonly recognized in April to August. We plan to discuss more detail of underlying physical processes, applying the three dimensional transformed Eulerian mean series formulated by Kinoshita and Sato (2013a, b) and Sato et al. (2013) to the output data of a gravity wave resolving general circulation model.

Keywords: gravity waves, tidal waves, mesosphere



## A study on a humidity estimation method using the side-lobe emission from a wind profiling radar

Shigeru Inaka<sup>1\*</sup>, Jun-ichi Furumoto<sup>1</sup>, Hiromu Seko<sup>2</sup>, Toshitaka Tsuda<sup>1</sup>, Hiroyuki Hashiguchi<sup>1</sup>, Masahito Ishihara<sup>3</sup>

<sup>1</sup>Research Institute of Sustainable Humanosphere, Kyoto University, <sup>2</sup>Meteorological Research Institute, <sup>3</sup>Education unit for Adaptation to Extreme Weather Conditions and Resilient Society, Kyoto University

This study aims to develop a new method to observe water vapor horizontal distribution using a side-lobe emission of the 1.3 GHz-band wind profiling radar (WPR). The phase delay of the received side-lobe emission is mainly due to the refractive index fluctuation along the propagation path. In the atmospheric boundary layer, the temporal and spatial non-uniformity of water vapor determines the refractive index fluctuation. Main scope of the study is to extract humidity information from the atmospheric phase delay of side-lobe emission from a WPR. Horizontal humidity distribution can be derived by the data assimilation into numerical prediction model.

The receiver system and data analysis algorithm were developed. A software radio, USRP N200 with an RX daughter board was employed to detect side-lobe emission received by an antenna. A Rubidium frequency standard and a 1 pps signal source of GPS receiver were used for accurate estimation of phase delay variation. The frequency stability of a crystal oscillator, which is generally employed for a reference frequency source of WPR, is insufficient for the accurate estimation. We proposed a new method to compensate the frequency uncertainty of WPR by using data of the additional receiver nearby the WPR site.

IQ data detected by USRP N200 are transferred to the control PC via Ethernet. The program written in IDL language extracts the temporal variation of the phase delay from the received IQ signal. In order to achieve good performance even in low SNR conditions, we developed an algorithm using STFT (Short-term Fourier transformation) aiming to remove noise in undesired frequency range.

The developed system is promising to derive humidity information from side-lobe emission from various WPRs such as the operational WPR network in Japan (WINDAS (WInd profiler Network and Data Acquisition System)).

**Keywords:** Wind Profiling Radar, estimation of horizontal humidity distribution, non-hydrostatic forecast model, software radio, side-lobe, water vapor

## Variations of scale height at F-region peak based on ionosonde measurements during solar maximum over the EIA region

Yu-Jung Chuo<sup>1\*</sup>

<sup>1</sup>Department of Information Technology, Ling Tung University

Scale height is an important parameter in characterizing the shape of the ionosphere and its physical processes. In this study, we attempt to examine and discuss the variation of scale height,  $H_m$  around the F-layer peak height during high solar activity at the northern crest of the equatorial ionization anomaly (EIA) region. The data analyzed in this investigation, including  $H_m$ , the bottomside profile parameter, the F2-layer maximum critical frequency, and its peak height are derived from ionograms recorded at Chung-Li ionosonde station (geographical coordinate 24.9°N, 121.1°E) in 1999.  $H_m$  exhibits a day-to-day and seasonal variation, with a greater average daily variation during daytime in summer. Furthermore, the diurnal variation of  $H_m$  exhibits an abnormal peak at pre-sunrise during all the seasons, particularly in winter. This increase is also observed in the F2-layer peak height for the same duration with an upward movement associated with thermospheric wind toward the equator; this upward movement increases the N2/O ratio and  $H_m$ , but it causes a decrease in the F2-layer maximum critical frequency during the pre-sunrise period. In addition, the results show a strong/weak correlation between the bottomside/equivalent slab thickness and  $H_m$  throughout the year. Furthermore, we present a comprehensive discussion of the physical processes regarding the variation of  $H_m$  during high solar activity periods.

Keywords: scale height, ionospheric physics, EIA, ionospheric dynamics

## Sporadic E detection with GPS TEC and estimation of its horizontal and vertical structure

Jun MAEDA<sup>1\*</sup>, Kosuke Heki<sup>1</sup>

<sup>1</sup>Dept. of Science, Hokkaido University

### Sporadic E

Ionosphere is often divided into three parts (layers) depending on its electron density. F-layer is the most ionized layer at the highest altitude of 130~500 km, followed by E-layer at 90~130 km and D-layer at 70~90 km. During the summertime in mid-latitude region in where Japan is located, sudden increase of electron density in E-region of ionosphere which is called sporadic E often occurs.

### Observations of sporadic E

Ionosonde has long been taking the main role of ionospheric and sporadic E observation for a long time, now we have another method to monitor ionosphere, that is, GPS (Global Positioning System) satellites. We used TEC (Total Electron Content) which is derived from L1/L2 phase data to detect the sudden increase of electron density caused by Sporadic E. With the expansion of GNSS (Global Navigation Satellite System) and the dense network of GEONET GPS receivers in Japan, it is possible to watch ionosphere more spatially than ever before.

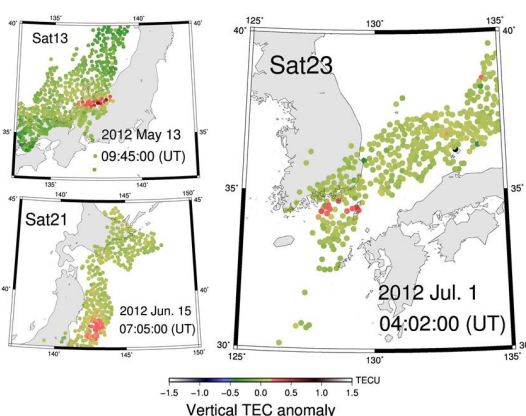
### Results of sporadic E observation with GPS TEC

We observed sporadic E with GPS TEC method which has mainly been used for ionospheric disturbances in F-region of ionosphere. This study provides first results of sporadic E observation with GPS TEC.

With the data from the dense array of GEONET GPS receivers, firstly, GPS TEC has revealed the horizontal structures of sporadic E. One of the characteristics of the horizontal structure of sporadic E is the East-West belt-like shape with the length of ~100 km and the width of ~20 km. Secondly, the results comes about sporadic E motion. The speed and the direction of sporadic E motion do not look uniform. Some sporadic E moves southwestward at the speed of ~50 m/s and some moves eastward at ~150 m/s.

We are also reporting the first results of thickness estimation of sporadic E with GPS TEC in combination with Ionosonde.

Keywords: Sporadic E, Ionosphere, GPS TEC, ionosonde, GEONET



## Estimation of spatial structure of sporadic E layer with 2-dimensional FDTD simulation

Taketoshi Miyake<sup>1\*</sup>, Takahiro Kurokawa<sup>1</sup>, Keigo Ishisaka<sup>1</sup>

<sup>1</sup>Toyama Prefectural University

We developed a 2-dimensional FDTD simulation code which can treat wave propagations in magnetized plasma. FDTD simulations can be performed with much less computer resources than those necessary for full particle simulations, in memories as well as cpu times. In this study, we performed FDTD simulations with different types of electron density profiles in the lower ionosphere, uniform ionospheric layer model and oval shape electron cloud model, and then confirmed characteristics of MF wave propagations in the lower ionosphere. We especially study on effects of wave frequencies. According to sounding rocket experiments, we can only obtain altitude profile of wave intensity, especially magnetic field intensity. In this study, therefore, we are going to try to estimate spatial structure in the lower ionosphere by analyzing altitude profile of magnetic field intensities of waves with various frequencies.

Simulation results indicate that spatial structure in the lower ionosphere can be estimated by analyzing altitude profiles of different waves emitted from different wave sources with various frequencies. Effects of spatial structure in the lower ionosphere are shown especially on propagation characteristics of MF waves above the altitude of the spatial structure itself. We are going to compare simulation results and results observed by S-310-40 sounding rocket, launched at Dec. 2011, and then estimate spatial structure of Es layer.

Keywords: Sporadic E layer, FDTD simulation, ionosphere, electron density profile, plasma wave propagation

## Observation of the wave-front structure of Es March 10, 2012 by VHF long-distance propagation

Takuya Yamahata<sup>1\*</sup>, Ichiro Tomizawa<sup>1</sup>

<sup>1</sup>Center for Space Science and Radio Engineering

We reported in the SGEPS-2012 meeting that the development of the Es-structure observation system in wide area by receiving VHF(VOR/ILS,108~118MHz) long-distance propagation signals as the Es wavefront structure moving in southward for the intense Es on March 10, 2012 around 12h JST[1]. We were analyzed the waveform data from 20 stations in the vicinity of the received field strength of Shanghai. We had derived the structure and movement of wide-area Es obtained by fitting a straight line to the peaks of field strength.

In the paper, we report the results of detailed analysis of the internal structure of the Es wavefront based on observed waveform.

At the first, we cut the data at 12 JST of two VOR station of higher S/N in the event to make a feature extraction by waveform correlation. In the same time, the presence of Es structure of more than 1000km has been confirmed with HFD, VHF band, Ionosonde, and the frontal Es has the moving speed of 92 m/s and the direction angle of 170 degree from north [2]. Since the duration of the Es front is 28 minutes, the entire width of the wave front could be confirmed with 163km. Since the entire wavefront is divided into two parts, it was found the presence of the entire half, 74 km structure. Further Analyzed the internal structure using cross-correlation, we were confirmed that Es has a width of about 14 km short wavefront structure ,since has a period of about 150 seconds It is similar to the value of the observations of Goodwin (1966) [3]. On the other hand, it was found that structure of peaks and troughs at intervals of 2 ~ 3km, this can be interpreted as a small structure less than the diameter of the Fresnel zone that is moving from the north to south direction.

Detailed analysis of other Es horizontal structures will be presented at the meeting.

### References

[1]Takuya Yamahata, Ichiro Tomizawa, and Mamoru Yamamoto: Development of Es-structure observation system in wide area by receiving VHF long-distance propagation signals, SGEPS 2012 Fall Meeting,

[2] Ichiro Tomizawa, Takuya Yamahata, Atsushi Yamamoto: Observation of large-scale structure and movement characteristics of Es by means of VHF long-distance propagation, SGEPS 2012 Fall Meeting,

[3]Goodwin: the dimensions of some horizontally-moving Es-region irregularities, Planet. Space Sci, vol.14, pp.758-771, 1966

Keywords: Es, VOR, ILS, VHF long-distance propagation, Sporadic E

## Accuracy improvement of reflection height and moving characteristics of frontal Es by oblique ionosonde and HF Doppler

Atsushi Ohtani<sup>1\*</sup>, Ichiro Tomizawa<sup>1</sup>

<sup>1</sup>SSRE, Univ. Electro-Comm.

The HF Doppler observation using 5006 and 8006 kHz transmitted from to the Chofu campus of UEC has been conducted at eleven stations including Sugadaira to observe of varieties ionosphere disturbances. However, it has the weak point that the wave reflection height cannot be specified by the HFD observation itself.

Fortunately, the distance between the HFD transmitting station (JG2XA) and the NICT Kokubunji ionosonde station is close to each other in only 8 km. Those Fresnel zones have an overlap area so that the two observations has the same reflection height. In this observation, we used a software defined radio receiver to receive ionosonde pulses from 7 to 9MHz around the 8006kHz HFD signal. The pulse transmission timing of ionosonde which is precisely scheduled in UTC were observed by mixing with the GPS synchronised 1sec pulse in the 1 micro-second accuracy. The propagation distance from Kokubunji to Sugadaira was measured by the arrival delay of ionosonde pulses. This method was applied to estimate the height and moving characteristics of Es. The reflection height can be determined from propagation distance and the reflection position of Es which were calculated from the movement speed and the direction angle through the HFD network. As the propagation path both to the ionosonde and the chofu HFD transmitter can be deduced by applying the method of Cornelius and Essex(1979) [1], we can deduce the same reflection height.

Around 20h JST(UT+9h) on July 28, 2012, the frontal Es with more than 200 km length passed over Sugadaira to Chofu by the speed of 60 m/s in the 182 degree from north was observed in this observation system. We obtained the accurate reflection height of the frontal Es as 115 km in matching the propagation path to the oblique ionosonde.

Acknowledgement: We are grateful to NICT for the ionosonde signal transmission.

### Reference

[1] D.W. Cornelius and E.A. Essex: Observations of mid-latitude sporadic E using the HF Doppler technique, J. Atmos. Terr. Phys., vol.41, no.5, pp.481-499, 1979.

Keywords: ionosphere, ionosonde, sporadic E

## Total electron content of plasmasphere and ionosphere before and after geomagnetic storm by using Quazi-Zenith satellite

Natsuki Kinugasa<sup>1\*</sup>, Fujinobu Takahashi<sup>1</sup>

<sup>1</sup>Yokohama National University

Quasi-Zenith satellite system (QZSS) is the regional navigation satellite system covering Japan and Oceania. Altitude of QZS is 32,000km at the perigee and 40,000km at the apogee. Thus, QZS observation is affected by both ionosphere and plasmasphere. Plasmaspheric contribution on QZS observations is considered to be different from that on GPS observations because altitude of GPS(global positioning system) satellite is 20,200km.

In this research, we're trying to measure QZS total electron content from dual-frequency propagation delay. And we will present the results of measured QZS- and GPS-TEC especially before and after geomagnetic storm.

Keywords: QZS, TEC, GPS

## Development of TEC observation method using small differences of arrival angles of geostationary-satellites

Takafumi Yokoyama<sup>1\*</sup>, Ichiro Tomizawa<sup>1</sup>, Michi Nishioka<sup>2</sup>, MAHO NAKAMURA<sup>1</sup>

<sup>1</sup>SSRE, Univ. Electro-Comm, <sup>2</sup>NICT

We have been observing Total Electron Contents (TEC) with the Faraday rotation method using positioning signals transmitted from geostationary satellites, ETS-VIII and MTSAT-2 [1]. On the other hand, to observe a slight change in angle of arrival when geostationary satellite positioning signal to pass through the ionosphere, caused by ionosphere refraction of radio wave propagation path, it can be converted into TEC values are known [2].

But most of all reports [3] do not argue about absolute values, but about fluctuations. In this study, to examine the relevance of numerical value between the Faraday and the angle-of-arrival methods, we set up the interferometer by the three parabolic antennas were installed at the intervals of 50 ~ 80 m as well as the Faraday measurement [4].

When we made a presentation last year, angle-of-arrival method was twice as Faraday method. So we re-examine a phase difference method between each antennas. And we recalculate orbital calculation. As a result, angle-of-arrival method was similar to Faraday method.

In addition, we compare QZS-TEC and IRI model with angle-of-arrival method. And we observed sporadic-E by arrival angle method. This result was same as GEONET in July 4th 2012. We speak these results.

### Acknowledgment

We can get QZS-data from Dr. Michi Nishioka. Thank you very much.

The study had received the support of NICT as an experimental project using ETS-VIII.

We can get GEONET data from Geospatial Information Authority of Japan. Thank you very much.

### Reference

[1] Takashi Uchiyama and Ichiro Tomizawa: Accuracy of verification absolute TEC measurement by the Faraday method ETS-VIII positioning signal, Society of Geomagnetism and Earth, Planetary and Space Sciences 2009.

[2] Kenneth Davies: Ionospheric Radio, IEE, 1990, pp.279-280, ISBN 0-86341-186-X.

[3] A.R. Webster and G.F. Lyon: The observation of periodic ionospheric disturbances using simultaneous Faraday rotation and angle of arrival measurements, J. Atmos. Terr. Phys., vol.36, no.6, pp.943-954, 1974.

[4] Takafumi Yokoyama and Ichiro Tomizawa: Development of TEC observation method using small differences of arrival angles of geostationary-satellites, Society of Geomagnetism and Earth, Planetary and Space Sciences 2012.

Keywords: Ionosphere, TEC, Faraday rotation method, Angle-of-arrival method, sporadic-E



## Frequency characteristics of the variations of ionospheric total electron content after earthquakes using 1-second TEC

Yuki Shimizu<sup>1\*</sup>, Hiroyuki Nakata<sup>1</sup>, Keigo Abe<sup>1</sup>, Toshiaki Takano<sup>1</sup>, Takuya Tsugawa<sup>2</sup>, Michi Nishioka<sup>2</sup>

<sup>1</sup>Graduate school of Engineering, Chiba University, <sup>2</sup>National Institute of Information and Communications Technology

There are many reports that ionospheric disturbances occur by giant earthquakes, such as the 2011 off the Pacific coast of Tohoku Earthquake. It is important to examine the ionospheric disturbance excited by earthquakes. Since this study is able to monitor the tsunami from satellites, and arise a social concern. Therefore, purpose of this study is examination of the ionospheric disturbances after earthquakes by frequency analysis of temporal variations of TEC observed by GEONET. In previous studies, frequency band have been limited to less than 15 mHz because of using 30-second GPS-TEC. While in this study we use 1-second GPS-TEC to examine high-frequency band temporal variations that can not examined by using 30 seconds GPS-TEC. We cover the earthquakes larger than M6.0 occurred in March 2011. We used GPS data where the elevation angle of satellites was larger than 30 degrees observed by 800 GPS receivers of GEONET. We derived a frequency characteristic of GPS-TEC by Fast Fourier Transform.

As a result, the variations by earthquakes are shown in two events over M6.5. We analyzed a frequency characteristics of the variations above the epicenters and 300km far from the epicenters. It is shown that the variation at 3.9 mHz and 4.9 mHz are observed above the epicenters in both events. These frequencies are close to those observed after the Pacific coast of Tohoku Earthquake, by using 30-seconds GPS-TEC.

Additionally, in Sanriku Earthquake on March 9 and the Pacific coast of Tohoku Earthquake on March 11, we detected the oscillation around 15 mHz and 20 mHz above the epicenter. It is thought that the variations at these frequency are not excited by the resonance in the neutral atmosphere that have ever been reported.

Keywords: ionosphere, TEC, earthquake, atmospheric gravity wave, acoustic wave

## Causal link of the seismic surface waves in the lithosphere and TEC perturbation in the ionosphere during the 2011 Tohok

Chia-Hung Chen<sup>1\*</sup>, Charles Lin<sup>1</sup>, Ruey-Juin Rau<sup>1</sup>, Akinori Saito<sup>2</sup>, Jann-Yenq Liu<sup>3</sup>

<sup>1</sup>Department of Earth Sciences, National Cheng Kung University, Tainan, Taiwan, <sup>2</sup>Department of Geophysics, Kyoto University, Kyoto, Japan, <sup>3</sup>Institute of Space Science, National Central University, Chung-Li, Taiwan

1Hz ground-based Global Positioning System (GPS) measurements from the Japan GOENT and Taiwan CWB are used to study the 2011 Mw 9.0 Tohoku earthquake at 05:46:23 UT on March 11, 2011. The high-rate GPS measurements can provide more detail information on the seismic fault of the earthquake. In this study, the propagation of seismic surface waves and ionospheric total electron content (TEC) perturbations generated by the Tohoku earthquake as well as their relationship are investigated by using the high-rate GPS measurements. It is found that the seismic surface waves and the initial ionospheric disturbances can transport from Japan to Taiwan. Results further found that there are time delay and deflection angle between the surface waves and the ionospheric disturbances when the earthquake waves transported from Japan to Taiwan. These results can help us to speculate the propagation path of the acoustic wave from the lithosphere to the ionosphere.

## Frequency dependence of the variations of total electron content associated with earthquakes

Keigo Abe<sup>1</sup>, Hiroyuki Nakata<sup>1\*</sup>, Toshiaki Takano<sup>1</sup>, Akinori Saito<sup>2</sup>, Takuya Tsugawa<sup>3</sup>

<sup>1</sup>Graduate School of Engineering, Chiba University, <sup>2</sup>Graduate School of Science, Kyoto University, <sup>3</sup>National Institute of Information and Communications Technology

Variations of total electron content (TEC) associated with earthquakes have been reported [e.g. Calias and Minster,1995; Afraimovich et al., 2001]. The common feature of the variations of TEC is periodic variations with a period of several minutes which is caused by the atmospheric gravity waves. On the other hand, the spatial scales of these variations are not clear. Dense GPS network system, such as GPS Earth Observation Network System (GEONET), is very useful for studying the special scales of the variations. In the 2011 off the Pacific coast of Tohoku Earthquake occurred on 11 March 2011, TEC fluctuations spreading from the epicenter was observed using GPS-TEC data determined by GEONET.[Tsugawa et al., 2011]. This clear variation of TEC is rarely observed. In this study, spatial scales of the spectral density of the GPS TEC variation is examined for the earthquakes ( $M > 6.0$ ) occurred in the inland and adjacent area of Japan during 2000. Ionospheric pierce points at the height of the 350 km are determined. FFT is applied to 32 minutes of TEC data obtained from GEONET receivers. As a result, the variation of TEC was observed near the epicenter of the earthquake ( $M > 6.8$ ) in 15 events out of 19 events. The variation in the frequency of 4.17 mHz is frequently observed in particular. This frequency is consistent with the resonance frequency of the atmosphere and earth. Thus, the main reason of the variation is probably acoustic waves generated by the displacement of the ground or tsunami by the earthquake. Next, the relationship between the displacement of the ground surface and TEC oscillations is examined. The displacement of the ground surface is calculated from their acceleration which was measured from the seismometers installed by NIED when the earthquakes were occurred in the inland. When the earthquakes occurred in sea area of Japan, the height of tsunami around the epicenter is estimated from the wave gauge settled by Japan Meteorological Agency. Considering the distance between the wave source and the ionospheric pierce point which show the maximum value of TEC variations,  $h'F2$  and  $foF2$ , the height of tsunami and the TEC variation are highly correlated each other. In addition, the propagation of TEC variations from the epicenter is observed in three events (the 2011 of the Pacific coast of Tohoku Earthquake ( $M9.0$ ), the Tokachi-oki Earthquake in 2003 ( $M7.4$ ), Kii-hantou Earthquake in 2004 ( $M7.4$ )). These three events are the top three tsunami heights. Considering that the TEC variations spread from the epicenter are due to gravity waves, it is estimated that the height of tsunami is correlated with the generation of the gravity waves. The variation of TEC is not correlated with the displacement of the ground surface in the earthquakes occurred in land or those without tsunami occurred in the sea. However, TEC variations are observed when the displacement of the ground near the source region is large. Therefore, the displacement of the ground is related to the variation.

Keywords: ionosphere, TEC, earthquake, atmospheric gravity wave, acoustic wave, FFT

## Effects of heavy weather conditions on the total electron content in the ionosphere: the case of typhoons

Hiroyuki Nakata<sup>1\*</sup>, Keigo Abe<sup>1</sup>, Toshiaki Takano<sup>1</sup>, Takuya Tsugawa<sup>2</sup>, Akinori Saito<sup>3</sup>

<sup>1</sup>Graduate School of Engineering, Chiba University, <sup>2</sup>National Institute of Information and Communications Technology, <sup>3</sup>Graduate School of Science, Kyoto University

Many researchers have reported that the total electron contents (TEC) are perturbed by earthquakes. It is known that the acoustic wave and/or atmospheric gravity wave excited by the ground perturbations cause the variations of TEC. This means that the variation of TEC can be excited by the other heavy weather conditions, such as Typhoon. In fact, in association with typhoon, the following perturbations are reported; foF2 anomaly (Rice et al., 2012), the electric field variation in high altitude of the ionosphere (Isaev et al., 2006), and TEC variation (Voeykov et al., 2008). Therefore, GPS-TEC variation above typhoons were determined in order to examine the effect of typhoons on the ionospheric electron density. GPS-TEC are derived from GEONET receivers installed by the Geospatial Information Authority of Japan. Since GEONET has constructed quite dense network of GPS receivers, the horizontal distribution of the TEC perturbation can be determined.

In this study, we selected strong typhoons (> Category 5). For example, Typhoon PRAPIROON (the 21st typhoon in 2002) generated in the south of Japan. Typhoon PRAPIROON moved northward and hit Kanto, Tohoku regions. When Typhoon PRAPIROON was crossing Japan, the enhancement of the power spectrum of TEC variations was observed. As the intensity of the typhoon was weaker, the intensity of the power spectrum also decayed. However, the intensity of the power spectrum was larger in the western side of typhoon eye, which is opposite of the wind intensity.

Keywords: Ionosphere, Total electron content, acoustic wave, atmospheric gravity wave, typhoon

## The Altitudinal Structure of Storm Enhanced Density observed by Space-borne and Ground-based GPS Receivers

Yukari Goi<sup>1\*</sup>, Akinori Saito<sup>1</sup>, Takuya Tsugawa<sup>2</sup>, Michi Nishioka<sup>2</sup>

<sup>1</sup>Kyoto University, <sup>2</sup>National Institute of Information and Communications Technology

The altitudinal structure of Storm Enhanced Density (SED) was studied using TEC data of the GPS receiver on GRACE satellite and the ground-based GPS receivers. SED is the high plasma density phenomenon which extends toward north-west direction from the equatorial ionization anomaly during geomagnetic disturbed times. The westward ExB plasma drift, which is driven by the poleward electric field in the sub-auroral region during the geomagnetic storm, causes the extended structure toward the west direction.

It is still not clear that the physical process of the transport of plasma from low-latitudes to high-latitudes. This carrying process could be attributed to the upward and poleward ExB drift, which is derived from the eastward electric field in low-latitude, and the diffusion along the geomagnetic line. The resultant velocity of two vectors, the ExB drift velocity and the diffusion velocity, would decide the extension of SED from low-latitude to high-latitude. When the ExB drift effect is stronger than the diffusion effect, the plasma of SED is lifted up by the ExB drift, after that the lifted plasma diffuses along the geomagnetic line at the altitude where the ExB drift velocity is zero. To clarify the physical process of the carrying out of plasma from low-latitude to high-latitude, we focus on the altitudinal distribution of the density structure of SED. GRACE-TEC data is the TEC data, which was derived from the GPS receiver on GRACE satellite, between GRACE satellite altitude and GPS satellite altitude. Two events of SED were observed simultaneously by MIT-TEC, which is the ground-TEC data on North-America continent, and GRACE-TEC during May in 2003. The amplitude of TEC enhancement was compared between GRACE-TEC and MIT-TEC.

In the first case, SED was observed in three orbital paths of GRACE satellite around 15LT on 21 May. The TEC enhancement of 20 TEC unit, which derived from SED, was observed in MIT-TEC in the first orbital path around 21UT. The TEC enhancement of 13 TEC unit was observed in GRACE-TEC at the same time and at the same location. In the second case, SED was observed in two orbital paths of GRACE satellite around 15LT on 29 May. The TEC enhancement of 30 TEC unit was observed in MIT-TEC in the first orbital path around 21UT. Similar results were obtained by the comparison using the other orbital path. These results indicate that more than 30 percent of TEC enhancement was observed above GRACE satellite. We will compare the amplitude of TEC enhancement using GRACE-TEC and MIT-TEC in 2003 so that the averaged altitudinal structure of SED would be obtained at every latitude. The balance between the upward and poleward ExB drift velocity, which was derived from the eastward electric field, and the downward diffusion velocity along the geomagnetic line would decide the altitudinal structure of SED.

Keywords: GPS, TEC data, ionosphere, Storm Enhanced Density

## A model of small scale field aligned currents in the middle and low latitudes as observed by the CHAMP satellite

Kunihito Nakanishi<sup>1\*</sup>, Toshihiko Iyemori<sup>2</sup>, Hermann Luhr<sup>3</sup>

<sup>1</sup>Department of Geophysics, Graduate School of Science, Kyoto University, <sup>2</sup>Data Analysis Center for Geomagnetism and Space Magnetism, Graduate School of Science, Kyoto University, <sup>3</sup>GeoForschungsZentrum, GFZ, Potsdam, Germany

We have reported that the magnetic field observation by the CHAMP satellite shows the ubiquitous existence of small scale (1 nT - 5 nT) magnetic fluctuations with period around a few tens seconds along the satellites orbit and they can be interpreted as the spatial structure of small scale field-aligned currents generated by the ionospheric dynamo driven by atmospheric gravity waves propagating from the lower atmosphere. The mechanism is as follows: First, the gravity waves generated by the lower atmospheric disturbance propagate to the ionosphere. Then the neutral winds oscillate causing the ionospheric dynamo, and the Pedersen and the Hall currents flow. Because the dynamo region is finite, the electric charge accumulates at the boundary of the finite dynamo region and causes polarized electric fields. The temporal change of the polarized electric fields makes them propagate along the geomagnetic field as the Alfvén wave, at the same time, the ionospheric currents divert to the field-aligned currents. The CHAMP satellite observes the spatial structure of the field-aligned currents generated in this way as a temporal change along the path.

We report a result of verification of the model compared with the observed data, in addition to physical quantities including the current and amplitude of the neutral wind oscillation estimated by the model using the data.

Keywords: spatial structure of field aligned currents, middle and low latitudes, the CHAMP satellite, atmospheric gravity wave, the lower atmospheric origin

## Low energy electron observation -over cusp region by LEP-ESA on Norwegian sounding rocket ICI-3

junpei takeshima<sup>1\*</sup>, Yoshifumi Saito<sup>2</sup>, Shoichiro Yokota<sup>2</sup>

<sup>1</sup>Department of Earth and Planetary Science, The University of Tokyo, <sup>2</sup>Institute of Space and Astronautical Science

The cusp region is a boundary between dayside and nightside magnetic field lines where solar wind directly enters into the ionosphere. E-t spectrogram of the precipitating electrons observed in the northward of the cusp region sometimes shows energy-time dispersion where high-energy electrons are observed earlier than low energy electrons. Kletzing et al.(2001) suggested that these precipitating electrons were accelerated at an altitude of thousand km by the field aligned electric field generated by Inertial Alfvén wave(IAW). Tanaka et al.(2005) also suggested that acceleration altitude was between 2000km and 6000km, and the observation agreed with the numerical simulation by assuming IAW model. According to the IAW model, the altitude where electrons are accelerated is different between the electrons with different energy.

ICI-3 sounding rocket was launched on 3 Dec 2012 from Svalbard, Norway and it succeeded in obtaining precious data in the RFC(Reverse Flow Channel) where plasma flow was opposite to the background convection in the high latitude ionosphere. Six science payloads including Fixed Bias Langmuir probe (FBL), Low Energy Particle experiment Electron Spectrum Analyzer (LEP-ESA), Multi-Needle&Sphere Langmuir Probe, AC/DC Magnetometer (ADM), Electric Field and Wave Experiment (E-field), and Sounding Rocket Attitude Determination System (SRADS) were on ICI-3. LEP-ESA measured the electron pitch angle distribution in the energy range between 10eV and 10keV with high time resolution of 11ms. During the flight, we repeatedly observed energy-time dispersion of the precipitating electrons that had time duration of about 1second. Different from the previously reported energy-time dispersion of the precipitating electrons where the dispersion was convex downward, most of the dispersion observed by ICI-3 LEP was convex upward. We have tried to understand the reason why the observed dispersion was convex upward. Assuming that the electrons with different energy are simultaneously accelerated, we have found that the higher the electron energy, the higher the acceleration altitude of the electrons. We will investigate if IAW model with some altitude distribution of the electron density can explain the observed dispersion that was convex upward.

Keywords: energy-time dispersion, Inertial Alfvén wave, acceleration Altitude

## Electron density perturbation near the Sq focus observed by S-310-37 sounding rocket

Manabu Shimoyama<sup>1\*</sup>, Takumi Abe<sup>2</sup>

<sup>1</sup>Nagoya University, Solar Terrestrial Environment Laboratory, <sup>2</sup>Japan Aerospace Exploration Agency, Institute of Space and Astronautical Science

The layers of anomalously high electron temperature are often observed near the Sq focus in winter hemisphere in lower E-region. Theoretical studies suggest that the electric potential near the center of the Sq focus in winter hemisphere is higher than that in summer hemisphere. The field-aligned electric field generated in lower E-region, where the electric conductivity is low compared with higher altitude, would accelerate electrons, and ambient electrons could be heated through direct collisional processes or plasma waves. The S-310-37 sounding rocket was launched to elucidate the generation mechanism of the electron temperature enhancement. Several electrostatic probes and electric field detector (EFD) were installed. Fast Langmuir Probe (FLP) and Electron Temperature Probe (TEL) were used to obtain the profiles of electron temperature and electron density with high time resolution. Fixed Bias Probe (FBP) is to detect fluctuations of electron density with high time resolution up to 800 Hz. Suprathermal Plasma Analyzer (SPA) aims to measure energy distribution function of thermal and suprathermal electrons and to verify the existence of electrons heated by accelerated electrons. EFD aims to measure three-dimensional electric field.

The rocket successfully passed near the Sq focus during the rocket upleg, and FLP and TEL identified the electron temperature enhancement around 95-100 km in altitude. Although some data were slightly contaminated or partly saturated due to unexpectedly large fluctuation of electron density, all instruments worked properly and obtained data successfully during the rocket flight. Electrostatic probes observed abrupt increase of electron density fluctuation at 95-100 km in the rocket upleg up to the rocket apogee of 138 km. According to FBP, the ratio of the fluctuated component to the background reached the maximum value 8% at 98 km. From analyses of FLP and SPA data, large fluctuation occurred at a specific rocket spin phase when the instrument faced toward the geomagnetic field which was connected to summer hemisphere. From these results, it is suggested that accelerated electrons along the geomagnetic field from summer to winter hemisphere may excite plasma waves through beam plasma instabilities, which was detected as an electron density fluctuation.

Keywords: sounding rocket, electron heating, beam plasma instability, lower E-region, electrostatic probe



## Changes of the electron temperature in the region of high electron with Fixed Bias Probe on the S-310-40 Sounding Rocket

Yusuke Yatsukawa<sup>1\*</sup>, ABE,Takumi<sup>2</sup>, MIYYAKE,Watary<sup>1</sup>

<sup>1</sup>Tokai University, <sup>2</sup>ISAS/JAXA

The electron temperature and electron density are important parameters as the basic characteristics of the ionospheric plasma, which has been observed by the sounding rocket, scientific satellite and ground-based radar for several decades. However, there are many unresolved problems about spatial distribution and temporal variation of the plasma. The S-310-40 sounding rocket was launched from Uchinoura Space Center at 23:48:00 on December 19, 2011 to investigate high-density plasma layer in the nighttime lower ionosphere, which can cause extra ordinal propagation of Medium Frequency radio wave. Among eight onboard instruments, Fixed Bias Probe (FBP) measures incident current to the probe in high time resolution, which is suitable to observe small-scale electron density perturbation. Fast Langmuir Probe (FLP) measures the current-voltage relationship of a cylindrical probe with a length of 200 mm and a diameter of 3 mm.

The electron density and temperature were derived from the current-voltage relationship through the rocket flight. The altitude profile of the electron density shows an existence of the high electron density layer at the altitude of ~100 km. A comparison with the ordinal sporadic E layer suggests that electron density inside the high density layer are not as large as sporadic E. The electron temperature inside the high density layer is observed to be 20 % lower than that in the surrounding region. In addition, the thickness of the layer is 2-3 times larger than the averaged thickness of the sporadic E layer. Therefore, the high density layer seems to have different feature compared to well-known sporadic E layer. In order to confirm this result and also to investigate the detailed energy distribution of electrons, we try to evaluate validity of fitting procedure to the current-voltage relationship obtained inside the high-density layer.

In the past, data points above the noise level in the probe current were used to estimate the electron temperature by evaluating a gradient of the electron current in the semi-logarithmic plot. The electron density was calculated by evaluating the electron saturation current in addition to a retarding region of the electron current. However, when the electron energy distribution is different from Maxwellian and has different gradient depending on the electron energy, the estimated temperature may be different from a real value. Therefore, we have tried to analyze a variation pattern of the electron current with the probe voltage in the retarding region. In this presentation, we report a result of the detailed evaluation and discuss an interpretation of the result.

## Electric field measurements in ionosphere by S-520-26 sounding rocket

Keigo Ishisaka<sup>1\*</sup>, Kousuke Suda<sup>1</sup>, Mamoru Yamamoto<sup>2</sup>, Takumi Abe<sup>3</sup>, Shigeto Watanabe<sup>4</sup>

<sup>1</sup>Toyama Prefectural University, <sup>2</sup>RISH, Kyoto University, <sup>3</sup>ISAS / JAXA, <sup>4</sup>Hokkaido University

S-520-26 sounding rocket experiment was carried out at Uchinoura Space Center (USC) in Japan at 5:51 JST on 12 January, 2012. The purpose of this experiment is the investigation of the bonding process between the atmospheres and the plasma in the thermosphere. S-520-26 sounding rocket reached to an altitude of 298 km 278 seconds after a launch. The S-520-26 payload was equipped with Electric Field Detector (EFD) with a two set of orthogonal double probes to measure both DC and AC less than 200 Hz electric fields in the spin plane of the payload by using the double probe method. One of the probes is the inflatable tube structure antenna, called the ITA, with a length of 5 m (tip-to-tip). And ITA is very lightweight (12.5g per one boom). The ITA extended and worked without any problems. It was the first successful use of an inflatable structure as a flight antenna. Another one is the ribbon antenna with a length of 2 m (tip-to-tip). The electrodes of two double probe antennas were used to gather the potentials which were detected with high impedance pre-amplifier using the floating (unbiased) double probe technique. The potential differences on the two main orthogonal axes were digitized using 16-bit analog-digital converter, sampled at 800 samples/sec with low pass filter at cut-off frequency of 200 Hz.

Results of measurements of DC electric fields by the EFD have the large sine waves that result from the payload rotation at the spin period. The largest contribution to the electric field measurements by double probes moving through the ionosphere at mid-latitudes is that due to the  $\mathbf{v} \times \mathbf{B}$  fields created by their motion across the ambient magnetic field, where  $\mathbf{v}$  is the rocket velocity in the Earth-fixed reference frame and  $\mathbf{B}$  is the ambient magnetic field. The sum of the squares of the two components represents the magnitude of the DC electric field in the spin plane of the payload. These data reveal abrupt, large-scale variations which can immediately be attributed to changes in the geophysical electric field since the  $\mathbf{v} \times \mathbf{B}$  fields are slowly varying. The sum of the squares data also reveals contributions at the spin frequency and its harmonics. These contributions result primarily from distortions of the waveforms in the raw data. Then we obtained three components of natural DC electric fields by subtracting the  $\mathbf{v} \times \mathbf{B}$  fields from raw data. As a result, the magnitude of DC electric field on a rocket orbit during the ascent was about 1mV/m, and the direction was for north-east.

Keywords: DC Electric Field, Ionosphere, Rocket experiment

## Measurement of propagation characteristics of MF band radio waves in lower ionosphere by S-310-40 sounding rocket

Keigo Ishisaka<sup>1\*</sup>, Tatsuya Fukazawa<sup>1</sup>, Takumi Abe<sup>2</sup>, Ken Endo<sup>3</sup>, Atsushi Kumamoto<sup>3</sup>, Takayuki Ono<sup>3</sup>

<sup>1</sup>Toyama Prefectural University, <sup>2</sup>ISAS/JAXA, <sup>3</sup>Tohoku University

The ionospheric D region is important in radio wave propagation because it absorbs energy from waves at MF, HF and VHF, and it reflects LF and VLF signals. Then D region is present only during daylight hours. Therefore, in the night-time, the MF band radio waves are propagated as far as an area where its radio waves cannot be propagated in the daytime. This reason why the radio waves cannot receive is that the D region is disappeared at night. However, the MF band radio waves that transmit from distant place have not been often received at the mid latitude in the night-time. In this time the sporadic E region cannot be observed by the ionogram. We guess that the D region appear in the lowest ionosphere like a daytime. To farther study the structure of the lowest ionosphere, we propose a method to measure the very low electron densities that occur at altitudes from 50 km to 90 km using the partial and perfect reflection characteristics of electromagnetic waves.

S-310-40 sounding rocket experiment was carried out at Uchinoura Space Center (USC) at 23:48 JST on 19 December, 2011. The purpose of this experiment is the investigation of characteristics of radio wave propagation in the ionosphere and the estimation of electron density structure in the lower ionosphere, when the intensity of radio wave measured on the ground will be attenuate at night-time. In order to measure the radio waves, a LF/MF band radio receiver (LMR) is installed on the sounding rocket. The LMR has measured the propagation characteristics of four radio waves at frequencies of 60 kHz (JJY signal from Haganeyama radio station), 405 kHz (NDB station from Minami-Daito), 666 kHz (NHK Osaka broadcasting station) and 873 kHz (NHK Kumamoto broadcasting station) in the region from the ground to the lower ionosphere. The LMR consists of a loop antenna, a pre-amplifier and a detector circuit. The loop antenna is set up in the nose cone, which is transparent to the LF/MF band radio waves, and is not deployed during the flight. Therefore, the LMR can measure the relative attenuation of radio waves from the ground up to the ionosphere. Furthermore three components of four radio waves measure by using three loop antennas. We can obtain the propagation directions of radio waves in the ionosphere directly.

We will explain a new radio wave receiver with the loop antenna system (LMR) on-board S-310-40 sounding rocket and show the results of propagation characteristics of radio waves in the ionosphere. And the approximate electron density profile can be determined from the comparison between propagation characteristics observed by the LMR and propagation characteristics calculated by the full wave method. The most probable electron density profile in the ionosphere is demonstrated in this study.

Keywords: Propagation characteristic of radio wave, Ionosphere, Rocket experiment

## Observation of the 2012 Geminids shower, and trial of meteor detection

Masayuki Toda<sup>1\*</sup>, Masa-yuki Yamamoto<sup>2</sup>, Yoshihiro Higa<sup>1</sup>, Yoshihiro Kakinami<sup>2</sup>, Daiki Kihara<sup>2</sup>, Junya Yamada<sup>2</sup>, Jun-ichi Watanabe<sup>3</sup>

<sup>1</sup>Nippon Meteor Society / Meteortrain Observation Team, <sup>2</sup>Department of systems engineering, Kochi University of Technology, <sup>3</sup>Public Relation Center, National Astronomical Observatory of Japan

Observation of meteors and meteor trains with a high sensitivity digital single-lens reflex camera was performed at Kiso observatory, University of Tokyo, from 13h43m to 20h39m UT on December 13, 2012. Single station observation was carried out there by using Nikon D3 and D4 digital cameras with lenses of 28 mm, f/1.4. The camera setting was ISO=25,600, shutter speed 1/1.3 seconds (0.769 s) with an interval of 1 s. As long as the capacity of CF cards allowed, continuous shooting of 1/1.3 s exposures was performed, resulting 24,868 frames recorded on Dec. 13. All of the images were checked frame by frame by viewing manually on the screen of PC, and meteors and relating meteor trains were picked up on the successive images. Many meteors and their meteor trains which belong to the Geminids was successfully detected from these images. Magnitude of the meteors and the meteor trains were determined in comparison with a star chart for visual meteor observation. The magnitude of a meteor and its meteor train is not absolute magnitude, but the apparent magnitude. The meteor train was divided into three parts and assumed the each range the upper end, the center, the bottom end, from the appearance side. The brightest part was determined from the three parts for each meteor and meteor train.

The number of appearances of the green short-duration meteor trains which is considered to be luminescence of OI 557.7 nm is counted. Observation of the meteor and meteor train by a high sensitivity digital single lens reflex camera was started in December, 2007. According to the peak day of main meteor showers, it is observing after it. Furthermore, development of an automatic meteor detection software which can discover a meteor from the huge number of pictures taken by quick repetition is also introduced in this paper.

### Reference

[1]Masayuki Toda, Masa-yuki Yamamoto, and Yoshihiko Shigeno, Measuring of short-duration meteor trains: altitude distribution of luminescence by double-station meteor observation with image intensified video cameras, Proceedings of Kochi University of Technology, Vol. 7, No. 1, 45-55, 2010.

(in Japanese, English Abstracts)

[2]Masayuki Toda, Observation of the a meteor train with the high sensitivity digital single-lens reflex camera, The Astronomical Herald, Vol.105, No.11, 716-718, 2012.

(in Japanese, Astronomical Society of Japan)

Keywords: Geminids, Meteor, Meteortrain, Meteor auto-detection software

## Development of notification system for bright meteor signals by using wide angle and time series images

atsushi iyono<sup>1\*</sup>, Naoki Wada<sup>1</sup>

<sup>1</sup>Dept. of Fundamental Science, Okayama University of Science

### 1. Purpose and Background

The Sky monitoring system by using wide angle lens camera have been maintained until Nov. 2011 at Okayama University of Science. Images are obtained by the CCD camera system which provide the slow shutter image, and they have been transferred to data storage PC system via the Internet connection. This system enables us to monitor the real time condition of the sky. We can now operate this system with 90% duty cycles. In the obtained images, bright meteors and sometimes fir balls were registered. Now we analysed these images by offline analysis software. In this report, we are going to describe our new system which can provide quick analysis results for meteor and fire ball at the moment of observations.

### 2. System

In the sky monitor system, CCD camera with wide angle (fish eye) lens and image server system have been operated in 24 hours/day. The exposure of CCD cameras has been set to 256 frames or 128 frames which correspond to 7 second or 4 second, respectively. The acquired image data have been stored in PC system via the internet ftp command. 28,800 images(500MB data size) are stored in each day. In offline mode, images are processed with contrast enhancement module, image differentiating and object detection module.

### 3. Development

In this researches, we develop new analysis system for online image processing and for providing meteor signal detection, arrival direction determination and brightness profile information. We are going to present new system and analysis result in this reports.

### Reference

K.Noguchi, "High-accuracy direction findings of meteors and development of an automatic meteor observation system by 5-channels radio interferometer", Kochi University of Technology, Graduate School of Engineering, 2009

Keywords: meteor, fire ball, image processing, simultaneous observation

## Optimization for airglow imaging in an urban area

Hidehiko Suzuki<sup>1\*</sup>, Shuka Sakurai<sup>1</sup>, Makoto Taguchi<sup>1</sup>

<sup>1</sup>Rikkyo University

An airglow imaging technique is a quite common and powerful tool for upper atmospheric study, since it can deduce horizontal wavelength and direction of phase propagation of atmospheric gravity waves. For example, a coordinated imaging observation by OMTI (Optical Mesosphere Thermosphere Imagers) system is conducted by Nagoya University in Japan. A combined field-of-view (FOV) of the imagers covers almost entire sky above Japan, and therefore, provides information about long traveling atmospheric waves such as ducted waves and TIDs [S. Suzuki et al., SGEPPSS Fall Meeting, 2012]. However, there is no airglow imager which has a FOV centered in the central part of Japan (Tokyo and Kanto area). The difficulty of airglow imaging in the urban area arises from strong contamination by artificial lights in the city. In particular light pollution is severe in the visible wavelength region which is also the most sensitive band for Si CCD device. However, luminosity of city light is relatively weak in the near infrared region (800~950 nm). Thus, imaging observation of some of the OH bands in this region can avoid the severe city light pollution. We performed spectra survey on both city lights and airglow during nighttime in the spectral region of 350~970 nm using a grating spectrometer in the central area of Tokyo (Ikebukuro). As a result we found that the OH7-3 band near 890 nm is the most adequate for an airglow imaging observation using a typical CCD sensor in the urban area.

Keywords: Airglow, Mesopause, OH airglow, Atmospheric gravity wave, spectroscopy

## Analysis of gravity waves observed by airglow imaging at Syowa Station (69S,39E), Antarctica

Takashi Matsuda<sup>1\*</sup>, Takuji Nakamura<sup>2</sup>, Mitsumu Ejiri<sup>2</sup>, Masaki Tsutsumi<sup>2</sup>, Kazuo Shiokawa<sup>3</sup>, Shin Suzuki<sup>3</sup>, Yoshihiro Tomikawa<sup>2</sup>

<sup>1</sup>The Graduate University for Advanced Studies, <sup>2</sup>National Institute of Polar Research, <sup>3</sup>Solar-Terrestrial Environment Laboratory, Nagoya University

Atmospheric gravity waves (AGWs), which are generated in the lower atmosphere, transport significant amount of energy and momentum into the mesosphere and lower thermosphere and cause the mean wind accelerations in the mesosphere. This momentum deposit drives the general circulation and affects the temperature structure. Airglow imaging is a useful technique for investigating the horizontal structures of AGWs at around 90 km altitude. However, observations of airglow imaging in Antarctica are very limited because of lack of observation sites. The Japanese Antarctic Research Expedition (JARE) has operated airglow imagers at Syowa Station (69S, 39E), Antarctica in 2002 and between 2008 and 2012.

Statistical analysis of image data in 2011 was performed. Observation was carried out from March to September at 139 nights, out of which 71 nights were with clear sky. We picked up 81 wave events in sodium images. Horizontal characteristics such as propagation directions, phase speeds, wavelengths, and observed periods were determined. Distributions of horizontal wavelength and observed period were similar to those obtained by imaging observations at middle and low latitudes, but the distributions of propagation direction and horizontal phase speed showed zonal anisotropy and seasonal variation.

The observed waves propagating eastward had faster phase speed (0m/s -150m/s) than those propagated westward (0m/s -60m/s) and faster waves (30m/s -150m/s) were only observed in July and August. The zonal anisotropy of the phase velocity distribution could be explained if wave sources are located at the eastward wind such as stratospheric polar night jet.

We will report analysis of the data in 2012 and discuss inter-annual variation of the phase velocity distribution and analysis using spectral techniques.

Keywords: atmospheric gravity wave, airglow imaging

## Statistical characteristics of MSTIDs using a 630-nm airglow imager at Magadan

Ryota Kumeno<sup>1\*</sup>, Kazuo Shiokawa<sup>1</sup>, Yuichi Otsuka<sup>1</sup>, Shin Suzuki<sup>1</sup>, Boris M. Shevtsov<sup>2</sup>, Igor Poddelsky<sup>2</sup>, Sergey Smirnov<sup>2</sup>

<sup>1</sup>Solar-Terrestrial Environment Laboratory, Nagoya University, <sup>2</sup>IKIR

Medium-Scale Traveling Ionospheric Disturbance (MSTID) is a wavy phenomenon in the ionosphere, which has a horizontal wavelength of 100-200 km and a period of a few hours. To date many observations of nighttime MSTIDs using all-sky airglow imagers have been conducted in Japan. Since OI 630-nm airglow emission is sensitive to the variation in the F-layer altitude and plasma density, 630-nm airglow images can monitor the two-dimensional structure of the MSTIDs. According to the previous studies, nighttime MSTIDs at Stecolny near predominantly propagate southwestward. However, their propagation characteristics at higher latitudes is still unclear. The Solar-Terrestrial Environment Laboratory, Nagoya University has made airglow imaging observations of MSTIDs in Magadan, Russia (60.1N, 150.7E), since November 2008, as part of the Optical Mesosphere Thermosphere Images (OMTIs) in collaboration with Institute of Cosmophysical Research and Radiowave Propagation (IKIR).

In the presentation, we will report statistics of MSTIDs over Magadan from January 2009 to August 2012 (630 nights). The ratio of clear-sky intervals to the total observations was 51% and data of 2149 hours of clear sky are available for the analysis.

Keywords: Medium-Scale Traveling Ionospheric Disturbance



## Thermospheric vertical wind and temperature observed by a Fabry-Perot imager

Kousuke Nakazaki<sup>1\*</sup>, Makoto Taguchi<sup>1</sup>, Yasunobu Ogawa<sup>2</sup>, Hidehiko Suzuki<sup>1</sup>

<sup>1</sup>Rikkyo University, <sup>2</sup>National Institute of Polar Research

Vertical wind and temperature in the mesopause and lower thermosphere were measured with a Fabry-Perot Imager (FPI) at Tachikawa, Tokyo. The FPI observed the OI 557.7 nm and OI 630.0 nm airglow. An all-sky camera (ASC) simultaneously observed OI 557.7 nm airglow. The data were obtained in the night of January 18/19, 2013, and reveal atmospheric gravity waves with periods of ~1 hour and vertical wind amplitudes of up to ~7 m/s. These values and the values obtained in the night of December 22/23, 2011 are consistent with past studies [cf. Mitchell and Howells, 1998] and the Cospar International Reference Atmosphere (CIRA-86). The FPI will be used in observations of slight perturbations in vertical wind and temperature due to gravity waves or local energy input in the auroral zone.

Keywords: lower thermosphere, mesopause, atmospheric gravity wave, Fabry-Perot imager

## Optimization of an etalon system for Rayleigh lidar daylight observations with an 82-cm telescope

Akihiro Yamamoto<sup>1\*</sup>, Taku D Kawahara<sup>1</sup>, Hidehiko Suzuki<sup>2</sup>, Makoto Abo<sup>3</sup>, Takuji Nakamura<sup>4</sup>, Mitsumu Ejiri<sup>4</sup>

<sup>1</sup>GSI, Shinshu University, <sup>2</sup>College of Science, Rikkyo university, <sup>3</sup>Tokyo Metropolitan University, <sup>4</sup>NIPR

A Rayleigh lidar to monitor atmospheric temperature from the troposphere to the mesosphere and upper clouds (PSC, PMC) in high altitudes was installed at Syowa Station in February January 2011 by the 52nd Japanese Antarctic Research Expedition (JARE 52). In the first season of the Syowa Rayleigh lidar observation, Polar Mesospheric Summer Echoes (PMSEs) observation by the lidar and the HF radar was successfully conducted [Suzuki et al. in prep]. A new receiver system of 35 cm telescope with a combination of a polarizer and an etalon was placed in Syowa by JARE 53 and started taking data. With this system, we confirmed an improvement of the signal to noise ratio by a factor of three. To detect weaker signal with an 82cm-telescope, an optimized etalon was simulated (air gap: 100 micrometer, reflection: 89%). In this presentation, we discuss this etalon and the expected signal to noise ratio.

Keywords: Syowa station, Rayleigh lidar, etalon, daytime observation

## Observations of three-dimensional structures of MLT wind fields based on meteor echo measurements using the PANSY radar

Masaki Tsutsumi<sup>1\*</sup>, Kaoru Sato<sup>2</sup>, Toru Sato<sup>3</sup>, Takuji Nakamura<sup>1</sup>, Akinori Saito<sup>4</sup>, Yoshihiro Tomikawa<sup>1</sup>, Koji Nishimura<sup>1</sup>, Hisao Yamagishi<sup>1</sup>, Takashi Yamanouchi<sup>1</sup>

<sup>1</sup>National Institute of Polar Research, <sup>2</sup>Graduate School of Science, The University of Tokyo, <sup>3</sup>Graduate School of Informatics, Kyoto University, <sup>4</sup>Graduate School of Science, Kyoto University

In this study we will develop a high quality meteor echo observation technique using the PANSY (Program of the Antarctic Syowa MST/IS Radar) system (47MHz) located at Syowa station (69S,39E), Antarctica. The radar started its initial observations in early 2011 and is currently operated for troposphere, stratosphere and mesosphere studies as one quarter system, being already the largest atmospheric radar in the Antarctic. The final configuration is to be an active phased array system with 1045 crossed-Yagi antennas, a peak transmitting power over 500kW and 55 digital receivers. By fully utilizing the versatility of the radar an unprecedented number of meteor echoes, that is, a few tens of times more echoes than that of conventional meteor radars, are expected. This will widen the possibility of meteor echo observation technique, which has been mostly limited to wind observations on a height profile basis, and enable the direct measurement of time-evolving three dimensional structures of wind and temperature fields in the polar mesosphere and lower thermosphere within a large horizontal area of about 500 km wide.

Keywords: MST/IS radar, Antarctic atmosphere, mesosphere, lower thermosphere, meteor echoes

## A study on development of statistical analysis system for variations of atmospheric environment

Ryota Hamaguchi<sup>1</sup>, Atsuki Shinbori<sup>2\*</sup>, Toshitaka Tsuda<sup>2</sup>

<sup>1</sup>Graduate School of Infomatics, Kyoto University, <sup>2</sup>Research Institute for Sustainable Humanosphere, Kyoto University

Integrated data analysis of various observations is important to understand the atmospheric environment, which requires cross-reference of data-base archived at different institutes. The Inter-university Upper atmosphere Global Observation NETwork (IUGONET) project has been conducted in FY 2009-2014 in order to enhance data exchange among the Japanese universities and research institutes. This project aims at establishing a meta-database system for ground-based observations as well as the data analysis software (UDAS). This thesis is concerned with development of the statistical analysis system as a part of UDAS, consisting of five functions as follows:

- (1) A test for the difference in the mean values between the two data distributions.
- (2) Cross-correlation coefficient and a test for non-correlation.
- (3) Analysis of coherence and phase for each frequency component.
- (4) S(Stockwell) transform analysis : Temporal variations of spectral density and dominant frequency for transient phenomena.
- (5) Trend test for the slope of a linear regression.

Because the sampling interval of observations is not always constant and missing data are sometimes included, a linear interpolation is adopted on the data before applying the statistical analysis system.

We applied this analysis system for the two meteor radars in Indonesia. The same radar systems are operated on the equator in west Sumatra and west Papua, Indonesia in 2003-2013. These data-sets are unique and useful to study longitude variations of the wind fields. First, we tested the altitude distribution of meteor echoes, and found no difference in the mean altitude, but a slight long-term trend. Frequency spectrum indicated that the quasi-two day wave is dominant at 90 km altitude for the meridional wind component, where the long-term envelope of the wave amplitudes correlated well between the two radars. This statistical analysis system can clarify trends and variations of atmospheric conditions. Therefore, it is expected to advance our understanding on the global changes as well as the effects of solar activities on the lining environment.

Keywords: IUGONET, analysis software, statistical test, frequency analysis, trend test, meteor radar

## Climatology of the middle atmosphere over Alaska in winter season: quantitative comparison with other indexes

Kazuyo Sakanoi<sup>1\*</sup>, Yasuhiro Murayama<sup>2</sup>, Richard L. Collins<sup>3</sup>, Kohei Mizutani<sup>2</sup>, Seiji Kawamura<sup>2</sup>

<sup>1</sup>Faculty of Arts and Sciences, Komazawa University, <sup>2</sup>National institute of Information and Communications Technology, <sup>3</sup>the Geophysical Institute, the University of Alaska, Fairbanks

Purpose of this research is to clarify climatology of the middle atmosphere over Alaska in winter season. This work includes analysis and discussion about the role of atmospheric waves which affects disturbance of the middle atmosphere and about the relationship between disturbance of the middle atmosphere and activities of solar and lower atmosphere. So far we analyzed Rayleigh lidar and MF radar data at Poker Flat Research Range (65.1N, 147.5W) in Alaska, which are conducted by NICT (National institute of Information and Communications Technology) and GI/UAF (the Geophysical Institute, the University of Alaska, Fairbanks), and stratospheric assimilation data provided by the United Kingdom Meteorological Office on a period that extends from November 1998 to April 2012, which period covers over one solar cycle of 11 years.

We derived the results listed below:

- \* Over ten major stratospheric sudden warmings (SSW) occurred during analyzed period.
- \* Before major SSWs temperature increasing of 10 - 30 K in the lower mesosphere was observed by the lidar.
- \* Just before major SSWs disappear of temperature peak as stratopause and temperature was almost constant from 40 - 80 km altitude range was seen in the results of two-event observations by the lidar.
- \* During major SSWs temperature decreasing of 10 - 20 K in the lower mesosphere was observed by the lidar at two events.
- \* Intermittent reversals of East-West wind were also observed by the MF radar at all major SSW events.
- \* At all major events East-West wind reversal (eastward to westward) from 30 - 90 km altitude range was seen by the MF radar observations. This wind reversal starts and descends from mesosphere to upper stratosphere and occasionally to troposphere.
- \* Remarkable elevation of the center altitude of middle atmosphere jet occurred in the 2003/2004, 2005/2006, 2008/2009 winters.
- \* The elevation of the stratopause (~ 55km to 70km) also observed in the 2003/2004 winter.

We compared occurrence time of these above and other phenomena which presented in papers during disturbed period in the Arctic middle atmosphere with the sun spot number and the QBO index in terms of SSW categorization. However, no clear relationship was found between occurrence time of disturbance in the Arctic middle atmosphere and two indexes. This results suggests that two SSW categorization, major or not, is not suited for quantitative comparison. Therefore we will do further analysis of the lidar and MF radar data, stratospheric assimilation data and some indexes in order to find most suitable value in quantitative comparison.

Keywords: Middle atmosphere disturbance, Atmospheric waves, Lidar, MF radar, Arctic region, Stratospheric sudden warming

## Improvement of Radio Acoustic Sounding System aiming to the operational meteorological instruments

Jun-ichi Furumoto<sup>1\*</sup>, Hiroyuki Hashiguchi<sup>1</sup>, Mamoru Yamamoto<sup>1</sup>, Toshitaka Tsuda<sup>1</sup>

<sup>1</sup>Research Institute for Sustainable Humanosphere, Kyoto University

Radio Acoustic Sounding System (RASS) is one of the most promising remote-sensing techniques to measure atmospheric temperature profile by combining a wind profiling radar and acoustic source. RASS has an advantage in the availability in the temperature measurement regardless the weather condition and day-and-night.

The reduction of noise from the ground-based acoustic source is very important subject to make a RASS measurement for practical use. Authors introduced the high-directional speaker system (LRAD-1000) into the RASS measurement of L-band wind profiling radar to reduce the noise pollution problem. LRAD-100 has very low side-lobe emission by combining DSP-controlled acoustics at two center frequencies. This paper demonstrates the performance of noise reduction and temperature measurements by applying LRAD-100 to L-band wind profiling radar.

The vertical resolution of RASS measurement is determined by the pulse-width of wind profiling radar. This paper also aims to improve the vertical resolution of RASS measurement to detect the distinct peak of inversion layers. We propose a new method to use oversampled data to obtain high-resolution temperature profile. The improvement of height resolution can be derived by extracting the information of overwrapped height from the over-sampled data. The results is presented in the paper.

Keywords: RASS, wind profiling radar, atmospheric temperature

## Primary observation results of potassium layer by a tunable resonance scattering lidar

Mitsumu Ejiri<sup>1\*</sup>, Takuo Tsuda<sup>1</sup>, Makoto Abo<sup>2</sup>, Taku D Kawahara<sup>3</sup>, Takuji Nakamura<sup>1</sup>

<sup>1</sup>National Institute of Polar Research, <sup>2</sup>Graduate School of System Design, Tokyo Metropolitan University, <sup>3</sup>Faculty of Engineering, Shinshu University

The National Institute of Polar Research (NIPR) is leading a six year prioritized project of the Antarctic research observations since 2010. One of the sub-project is entitled "the global environmental change revealed through the Antarctic middle and upper atmosphere". Profiling dynamical parameters such as temperature and wind, as well as minor constituents is the key component of observations in this project, together with a long term observations using existent various instruments in Syowa, the Antarctic (39E, 69S). As one of instruments in this project, we are developing a new resonance scattering lidar system with multiple wavelengths and plan to install and operate it at Syowa (69S), Antarctica. The lidar transmitter is based on injection-seeded, pulsed alexandrite laser for 768-788 nm (fundamental wavelength) and a second-harmonic generation (SHG) unit for 384-394 nm (second harmonic wavelength). The laser wavelengths are tuned in to the resonance wavelengths by a wavemeter that is well calibrated using a wavelength-stabilized laser. The lidar will measure temperature profiles using resonance scatter of atomic potassium (K, 770 nm) and density variations of minor constituents such as atomic iron (Fe, 386 nm) and K, calcium ion (Ca<sup>+</sup>, 393 nm), and aurorally excited nitrogen ion (N<sub>2</sub><sup>+</sup>, 390-391 nm). Currently, the laser pulses are transmitted with approximately 120 mJ/pulse at 25 Hz and the backscattered signal is received with a 35 cm diameter telescope. We got the first light from the K layer on January 28, 2013 and have started test operation to measure K density profiles at National Institute of Polar Research in Tachikawa. We will show the primary observation results and discuss nightly variations of K densities.

Keywords: resonance scattering lidar, mesosphere lower thermosphere, tunable, Potassium

## Optical axis alignment between laser light and a receiver for a resonant scattering lidar observation

Taku D Kawahara<sup>1\*</sup>

<sup>1</sup>Faculty of Engineering, Shinshu University

A method of laser light and a telescope alignment for a resonant scattering lidar is typically done by monitoring signal with an oscilloscope. The temporal signal intensity variation is seen on the screen when the screening is triggered by laser shots. In the case of a sodium lidar, we typically confirm the signal around 90 km which is all by resonant scattering. However, the method depends on how clearly one can see the signal from the Na layer. In this talk, a more practical alignment method is presented by watching not Na signal but Rayleigh signal.

Keywords: resonant scattering, lidar, laser, field of view alignment



## Preliminary results of multi-direction lidar system experiments

Wataru Muranaka<sup>1\*</sup>, Taku D Kawahara<sup>1</sup>, Satonori Nozawa<sup>2</sup>

<sup>1</sup>Faculty of Engineering, Shinshu University, <sup>2</sup>STE Lab., Nagoya University

Shinshu University, Nagoya University and RIKEN developed an all solid-state, high-power Na lidar for the temperature/wind measurements in the MLT region over EISCAT radar site in Tromso (69N), Norway. The lidar has a higher power (~4W@589nm) compared with other Na lidars. This high power laser enables us to acquire the data with quite high temporal resolution (~3 min), even if we use a standard size telescope (35 cm diameter). This suggests a new observation method like a scanning lidar using a multi-direction telescope such as Meade LX200-ACF35. The laser transmitter has two rotary stages, which are horizontally/vertically placed. Two 45-degree mirrors are on each rotation axis which enable laser to transmit all the direction. In this talk, we show some preliminary results of directing laser and the telescope.

Keywords: sodium, lidar, three dimensional